High-Power Sub-300-Femtosecond Quantum Dot Semiconductor Disk Lasers

Cesare G. E. Alfieri, Dominik Waldburger, Matthias Golling, and Ursula Keller

***Abstract*— Self-assembled quantum dots (QDs) as active media for ultrafast semiconductor disk laser offer large gain bandwidths, fast gain dynamics, and high temperature stability. We report on the shortest pulses and the highest pulse peak power from an optically pumped vertical external cavity surface emitting laser (VECSEL) based on QDs and optimized for passive modelocking at 1035 nm using a semiconductor saturable absorber mirror. We demonstrate 216-fs pulses with an average output power of 269 mW at a pulse repetition rate of 2.77 GHz and 396 W peak power. At a lower pulse repetition rate of 1.67 GHz, we achieve 193-fs pulses with 112 mW of average output power. We remark a higher optical-to-optical pump efficiency compared to our previous QW VECSELs in the sub-300-fs regime. This is further confirmed by a comparative analysis of the saturation recovery which reveals longer carrier lifetimes for the QD compared to QW VECSELs.**

***Index Terms*— Mode locked lasers, quantum dots, semiconductor disk lasers, vertical-external cavity surface-emitting lasers, ultrafast optics.**

I. Introduction

ULTRAFAST optically pumped semiconductor disk lasers (SDLs) [1], [2] are interesting for many applications such as dual comb spectroscopy [3] and multiphoton microscopy [4]. SDLs can operate within a large spectral range with high-power emission and diffraction-limited output beams. In particular, vertical external cavity surface-emitting lasers (VECSELs) [5] passively modelocked with semiconductor saturable absorber mirrors (SESAMs) [6], [7] and the more compact modelocked integrated external cavity surface-emitting laser (MIXSEL) [8] have shown considerable improvements during the last years in terms of output power and pulse duration [9], [10]. To date, the best ultrafast SDLs in terms of average output power and pulse duration use InGaAs quantum wells (QWs) for both gain and absorber structures and operate close to a center wavelength of 1 μm. Although QWs offer high density of states (DOS) for high modal gain and moderately large emission bandwidth, we recently have demonstrated with our results that a significantly reduced gain saturation fluence due to spectral hole burning limits the maximum pulse energy in the femtosecond pulse duration regime [10]. Furthermore, the short carrier lifetime in highly inverted QWs reduces the optical-to-optical pump efficiency to typically $\approx 0.5\%$ in the sub-300-fs pulse duration regime [1], [2]. In fact, the electron-hole pairs (created by the continuous pumping) spontaneously recombine in the QW before they can be used for pulse amplification. Additionally, the strong temperature dependence of emission and absorption spectra represents a serious technological challenge for fully QW-based MIXSELs, where two different QW designs need to be carefully calibrated to compensate the temperature gradient between gain and absorber regions inside the epitaxial structure [11].

In contrast, self-assembled quantum dots (QDs) offer a number of fundamental benefits for ultrafast SDLs such as broad and flat gain bandwidth, low lasing threshold, very fast gain dynamics owing to the stronger spatial confinement and extended wavelength range with no need of strain compensation layers even though they have a reduced DOS [12]–[15]. Furthermore, the high degree of freedom in the growth process can lead to engineered QDs with greatly reduced temperature sensitivity [16], [17] and longer carrier lifetimes [18]. To date, QD-based SDLs in continuous wave (cw) operation achieved wavelength tuning up to 69 nm [19] and output powers up to 8.4 W [20]. With SESAM modelocking, the shortest pulse duration of 416 fs was achieved with 143 mW of average output power using a QD SESAM [21]. Here we report a significant further improvement of SESAM-modelocked QD VECSELs pushing the pulse duration into the sub-300-femtosecond regime while still maintaining an average output power of more than 250 mW.

II. Growth and Characterization

The QDs used in this work are based on Stranski-Krastanov (SK) growth formation technique. Each QD layer consists of a sevenfold deposition at 480°C of 0.1 nm InAs and 0.1 nm $In_{0.2}Ga_{0.8}As$, for a total nominal thickness of 1.4 nm and an average 60% indium. The room-temperature photoluminescence (PL) spectrum of the self-assembled QDs is centered at 1025 nm. The large QD-size variation results in a broad 135-nm full width at half maximum (FWHM) bandwidth, which is almost 100 nm broader compared to the PL emission of the QWs used for our recent 100-fs VECSELs (Fig. 1a) [9]. The comparison between the absorptions of a QW-based and a QD-based SESAM performed at 30°C and 70°C confirms the expected lower temperature sensitivity of the self-assembled QDs. We measure an absorption temperature shift of $\approx$ 0.17 nm/K for the QDs, in comparison $\approx$ 0.32 nm/K

Manuscript received December 21, 2017; revised January 27, 2018; accepted January 29, 2018. Date of publication February 1, 2018; date of current version February 22, 2018. This work was supported by the D-A-CH Program with the QD-MIXSEL Project, which was scientifically evaluated by the Swiss National Science Foundation and the Deutsche Physikalische Gesellschaft. *(Corresponding author: Cesare G. E. Alfieri.)*

The authors are with the Department of Physics, Institute for Quantum Electronics, ETH Zürich, 8093 Zürich, Switzerland (e-mail: calfieri@phys.ethz.ch; dominikw@phys.ethz.ch; golling@phys.ethz.ch; keller@phys.ethz.ch).

Color versions of one or more of the figures in this letter are available online at http://ieeexplore.ieee.org.

Digital Object Identifier 10.1109/LPT.2018.2801024

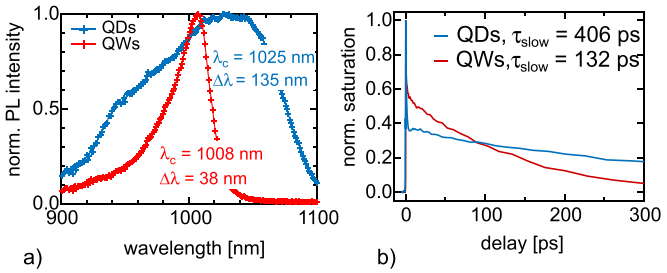

Fig. 1. a) Photoluminescence (PL) at room temperature of InGaAs QWs and SK QDs. b) Transient of the saturation of SK QDs and InGaAs QWs. The QDs clearly exhibit a slower recovery time which improves the optical-to-optical pump efficiency.

for the QWs. We use a degenerate pump-probe setup with a center pump-probe wavelength of 1010 nm and 130-fs pulses at the sample position to measure the saturation recovery of the SK QDs. With this technique, we measure a signal proportional to the instantaneous carrier population in the active layers, therefore taking into account radiative and non-radiative recombination. For this reason, we obtain lifetimes significantly shorter than the nanosecond timescale usually measured for only radiative lifetimes [18]. In particular, we obtain for the QDs a slow component of the recovery time of 406 ps which is significantly longer than the 132-ps measured in [10] for QWs (Fig. 1b). This longer saturation recovery time is obtained with reduced non-radiative losses and results in a higher optical-to-optical pump efficiency [10], [22].

The VECSEL structure is designed for operation around 1035 nm. The laser light is reflected by a 23.5-pair AlAs-GaAs distributed Bragg reflector (DBR). The active region consists of 16 QD layers embedded in pump-absorbing GaAs barriers and positioned in pairs with 50-nm separation on adjacent sides of the antinodes of the standing wave pattern (Fig. 2a). Atomic force microscope (AFM) measurements of uncapped QD islands reveal that the lattice constant mismatch of the InGaAs layer with the underlying GaAs causes the formation of pyramidal SK QDs with 2-4 nm height and 20 to 40 nm width (Fig. 2b). The average enhancement of the standing electric field intensity pattern in the QD active layers is kept at the rather high value of 0.71 (normalized to 4 outside the fully reflective structure) to increase the small signal gain and partially compensate the lower gain cross section of SK QDs compared to QWs. The increased gain, however, reducesthe gain bandwidth and decreases the gain saturation fluence [23] (Fig. 2d) introducing a trade-off that needs to be optimized for different operation parameters. A final anti-reflection (AR) section combines five alternating layers of AlAs and $Al_{0.15}Ga_{0.85}As$ and a single layer of silicon oxide (SiOx). The AR section is optimized to reduce the pump reflection at 808 nm and ensure a flat and low structural group delay dispersion (GDD) below ± 100 fs^2 over a bandwidth of $\pm$ 20 nm around the lasing center wavelength (Fig. 2c).

The VECSEL chip is grown in reverse order on an undoped GaAs (100) substrate with a molecular beam epitaxy (MBE) for subsequent flip-chip bonding.

The etch-stop layer, the anti-reflection section and the DBR are grown at 620°C while the GaAs barriers in the active

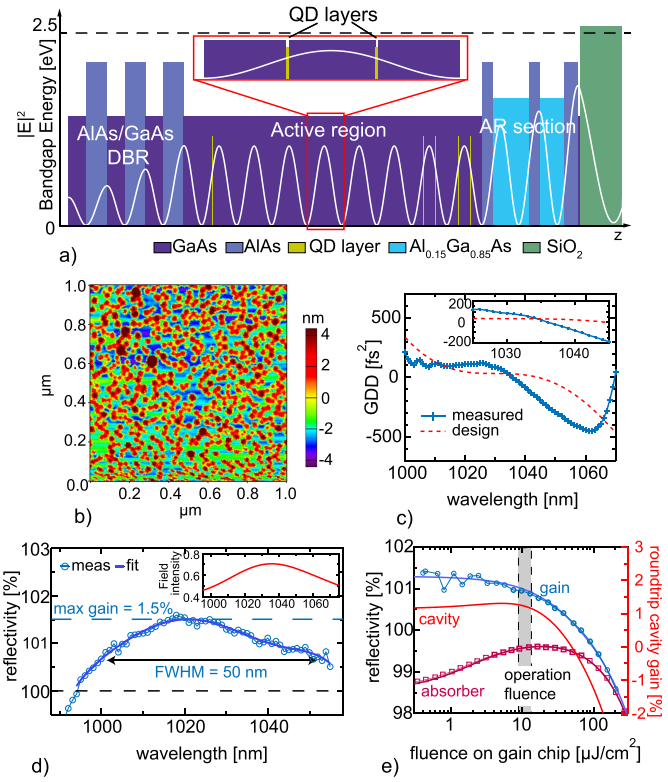

Fig. 2. a) Epitaxial structure of the QD VECSEL with the standing wave intensity profile at the center wavelength of 1035 nm (white curve). b) Atomic force microscope (AFM) picture of the surface of a SK QD layer. c) Measured and designed dispersion of the VECSEL chip. The measurement is performed at room temperature and normal incidence. Inset: zoom around the lasing center wavelength. d) Spectral gain of the QD VECSEL, measured at -10°C at a pump intensity of 25 kW/cm^2. Inset: designed average field intensity in the QD layers, peaked at 1035 nm. e) Nonlinear reflectivity measurements (markers) and fits (solid line) of the gain and absorber elements in the VECSEL cavity. The red solid line represents the roundtrip cavity gain, taking into account that a V-shaped cavity produces a double pass on the gain chip and a single pass on the absorber per roundtrip. The laser operation point is slightly shifted into the rollover of the roundtrip cavity gain.

region are grown at 580°C. After growth, the chip is Indium soldered onto a 5×5 mm, 1 mm thick CVD diamond heat spreader and the GaAs substrate is removed through wet etching. The final layer is deposited with plasma enhanced chemical vapor deposition (PECVD). The difference between the measured and designed GDD profile (Fig. 2c) can be explained by the epitaxial growth errors and deviations from the nominal optical thickness ($\pm$1%). Nevertheless, we reach a flatness of ± 200 fs^2 over a bandwidth of ± 10 nm around the designed lasing center wavelength.

The optical gain of the VECSEL chip is characterized with the setups described in [24] and probed with small sub-20 μm spot sizes. Under an optical pump intensity of 25 kW/cm^2 (total pump power $\approx$ 2 W) and a heatsink temperature $T_{HS} = -10$°C, the spectrally resolved reflectivity shows a maximum small signal gain of 1.5% at 1020 nm and a broad gain bandwidth of more than 50 nm (Fig. 2d).

Under the same conditions, the fluence-dependent gain saturation is probed at 1035 nm with 170-fs pulses. We measure a small signal gain of 1.3% and a saturation fluence of

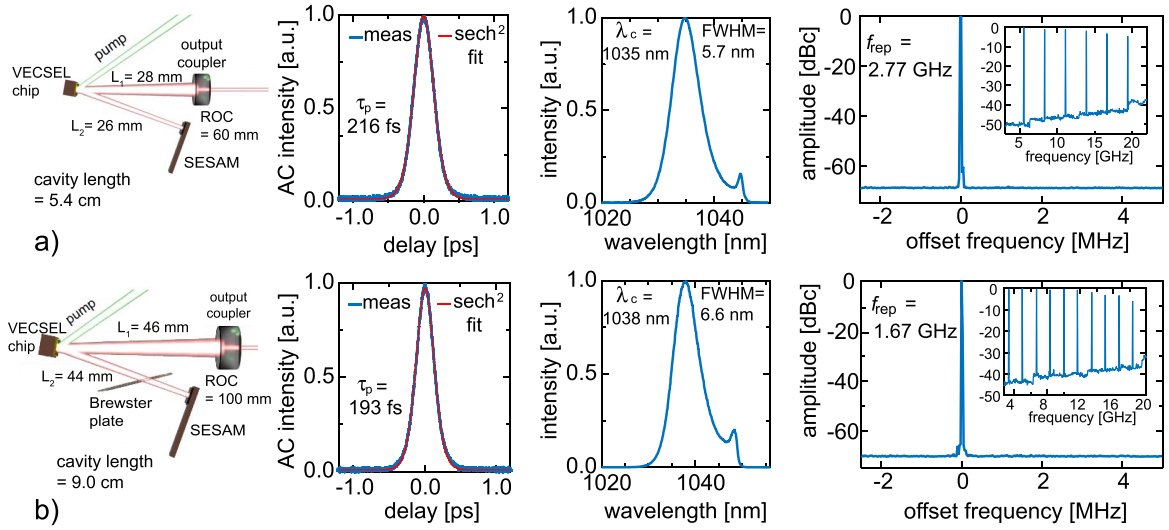

Fig. 3. SESAM modelocked VECSEL generating pulses as short as (a) 216 fs and (b) 193 fs. For both results we show the cavity design, the non-collinear SHG autocorrelation trace, the optical spectrum and the microwave spectrum with a high signal-to-noise ratio of 70 dB (resolution bandwidth of 1 kHz). Inset: long span of the microwave spectrum (resolution bandwidth of 300 kHz) showing that all the harmonics of the pulse repetition rate are present with equal power. A side peak appears on the right side of the optical spectrum, probably due to a non-flat OC rate combined with a smaller SESAM modulation at higher wavelengths.

37.6 μJ/cm^2 (Fig. 2e). We observe that despite the higher average field intensity in the QDs, the saturation behavior is comparable to state-of-the-art ultrafast QW VECSELs, but the small signal gain is roughly twice as low [9].

III. Modelocking Results

The SESAM used for modelocked operation consists of a standard MBE-grown single InGaAs QW absorber embedded in AlAs barriers on top of a 30-pair GaAs/AlAs DBR and top-coated with a $\lambda/4$ Si_3N_4 layer [25] Low-temperature MBE growth at 280°C was chosen to provide both a sufficiently fast saturable absorber as required for femtosecond pulse generation and still preserving a low nonsaturable loss of 0.1%. At 1035 nm and 22°C heatsink temperature the measured saturation fluence is 4.6 μJ/cm^2 and the modulation depth is 1.4% (Fig. 2e).

The laser resonator is based on a standard V-shaped cavity with 20° angle between the two cavity legs. A curved output coupler (OC) and the SESAM are used as end mirrors and the gain structure forms the folding mirror (Fig. 3a). The OC has a radius of curvature (ROC) of 60 mm and a transmission of 1.2% at 1035 nm. The distance between VECSEL and OC is set to 28 mm while the second cavity leg is 26 mm. For a stronger absorber saturation, the resonator mode on the gain chip is designed to be roughly twice as large as on the SESAM (i.e. a 139 μm and 73 μm radius, respectively). The VECSEL chip is pumped at 45° with an 808-nm low-brightness diode laser and the pump spot is shaped to be circular with 130 μm radius on the gain chip's surface. During operation, the VECSEL chip and the SESAM are temperature stabilized to −19°C and 24.5°C respectively. At a pump power of 13 W, we obtain a Gaussian output beam with $M^2 < 1.1$ and stable fundamental modelocking operation confirmed by a detailed pulse characterization (Fig. 3a). The measured optical spectrum is centered at 1035 nm, with a FWHM bandwidth of 5.7 nm and the autocorrelation trace, fitted to a sech^2 pulse shape, reveals a pulse duration of 216 fs. With an average output power of 269 mW at a repetition rate of 2.77 GHz, the VECSEL generates a record-high pulse peak power of 396 W for a QD SDL. Finally, an optical-to-optical efficiency of 2.1% makes this QD VECSEL the most efficient compared to any other sub-300-fs SDL. As observed before with QW SDLs [26], [27] and other SESAM-modelocked lasers such as high-power Yb-doped thin disk lasers [28], the QD VECSEL operates just in the rollover of the roundtrip cavity gain (Fig. 2e). Further increase of the pump power pushes the laser from clean fundamental modelocking to multiple pulses per cavity roundtrip.

The same VECSEL chip and SESAM, again temperature stabilized to −19°C and 24.5°C respectively, are tested in a longer cavity with a different OC (i.e. 100-mm ROC and 0.7% output coupling at 1035 nm) (Fig. 3b). In this case, the pump spot radius is increased to 177 μm and we obtain larger laser mode radii on the gain and on the absorber of 184 μm and 92 μm respectively. An additional 1 mm thick fused silica wedged Brewster plate is inserted into the cavity to add a small amount of positive cavity GDD ($\approx$ 64 fs^2) to obtain shorter pulses [23] (Fig. 3e). With this cavity configuration, we pushed the pulse duration into the sub-200-fs regime. At a pulse repetition rate of 1.67 GHz, we obtain 193-fs pulses that represent the shortest pulses from a QD VECSEL to date. The optical spectrum is centered at 1038 nm with 6.6 nm FWHM bandwidth (Fig. 3b). However, the non-perfect surface smoothness on the chip introduces a decreased average gain for larger cavity modes. Furthermore, the extra losses introduced by the intracavity Brewster plate and the more considerable thermal load on the structure compared to the previous experiment reduce the average output power to 112 mW at 23.7 W of optical pump power.

With a 306-Wpeak power, however, the performance is still comparable to previous QW VECSELs [9], [29]. The lower gain provided by QDs and the not perfectly optimized GDD profile are preventing the current QD VECSEL to reach the record short-pulse performance demonstrated for QWs in [9].

IV. Conclusion

To summarize, we have pushed SESAM-modelocked QD VECSELs to a new level of performance reporting sub-200 fs operation and the highest pulse peak power from a QD VECSEL together with the highest optical-to-optical efficiency for any sub-300-fs SDL. We confirm that QD gain media offers an attractive alternative to QWs for ultrafast SDLs, with some clear advantages for future applications and devices. We expect that especially the MIXSEL technology platform could greatly benefit from the QD temperature stability. We show that a longer carrier lifetime in the QD gain directly translates into a higher optical-to-optical pump efficiency. Currently further power scaling is limited by the larger mode size requirement in modelocked SDLs due to surface defects and heat dissipation. Further improvements towards kW peak power performance can be expected to be obtained with better optimized GDD and field intensity profiles, increased number of QD layers for increased gain and better surface quality.

Acknowledgment

The authors acknowledge support of the technology and cleanroom facility FIRST of ETH Zurich for advanced micro- and nanotechnology. The authors acknowledge funding within the D-A-CH program with the QD-MIXSEL project, which was scientifically evaluated by the Swiss National Science Foundation (SNSF) and the Deutsche Physikalische Gesellschaft (DPG).

References

[1] B. W. Tilma *et al.*, "Recent advances in ultrafast semiconductor disk lasers," *Light Sci Appl*, vol. 4, p. e310, Jul. 2015.

[2] M. Guina, A. Rantamäki, and A. Härkönen, "Optically pumped VECSELs: Review of technology and progress," *J. Phys. D, Appl. Phys.*, vol. 50, no. 38, p. 383001, 2017.

[3] S. M. Link, D. J. H. C. Maas, D. Waldburger, and U. Keller, "Dual-comb spectroscopy of water vapor with a free-running semiconductor disk laser," *Science*, vol. 356, no. 6343, pp. 1164–1168, 2017.

[4] F. F. Voigt *et al.*, "Multiphoton *in vivo* imaging with a femtosecond semiconductor disk laser," *Biomed. Opt. Exp.*, vol. 8, no. 7, pp. 3213–3231, 2017.

[5] M. Kuznetsov, F. Hakimi, R. Sprague, and A. Mooradian, "High-power (>0.5-W CW) diode-pumped vertical-external-cavity surface-emitting semiconductor lasers with circular TEM_{00} beams," *IEEE Photon. Technol. Lett.*, vol. 9, no. 8, pp. 1063–1065, Aug. 1997.

[6] U. Keller *et al.*, "Semiconductor saturable absorber mirrors (SESAM's) for femtosecond to nanosecond pulse generation in solid-state lasers," *IEEE J. Sel. Top. Quantum Electron.*, vol. 2, no. 3, pp. 435–453, Sep. 1996.

[7] U. Keller and A. C. Tropper, "Passively modelocked surface-emitting semiconductor lasers," *Phys. Rep.*, vol. 429, no. 2, pp. 67–120, Jun. 2006.

[8] D. J. H. C. Maas *et al.*, "Vertical integration of ultrafast semiconductor lasers," *Appl. Phys. B, Lasers Opt.*, vol. 88, no. 4, pp. 493–497, 2007.

[9] D. Waldburger *et al.*, "High-power 100 fs semiconductor disk lasers," *Optica*, vol. 3, no. 8, pp. 844–852, 2016.

[10] C. G. E. Alfieri *et al.*, "Optical efficiency and gain dynamics of modelocked semiconductor disk lasers," *Opt. Exp.*, vol. 25, no. 6, pp. 6402–6420, 2017.

[11] M. Mangold, M. Golling, E. Gini, B. W. Tilma, and U. Keller, "Sub-300-femtosecond operation from a MIXSEL," *Opt. Exp.*, vol. 23, no. 17, pp. 22043–22059, 2015.

[12] T. D. Germann *et al.*, "Quantum-dot semiconductor disk lasers," *J. Cryst. Growth*, vol. 310, no. 23, pp. 5182–5186, Nov. 2008.

[13] D. Bimberg, N. Kirstaedter, N. N. Ledentsov, Z. I. Alferov, P. S. Kop'ev, and V. M. Ustinov, "InGaAs-GaAs quantum-dot lasers," *IEEE J. Sel. Topics Quantum Electron.*, vol. 3, no. 2, pp. 196–205, Apr. 1997.

[14] J. Gomis-Bresco *et al.*, "Impact of coulomb scattering on the ultrafast gain recovery in InGaAs quantum dots," *Phys. Rev. Lett.*, vol. 101, no. 25, p. 256803, Dec. 2008.

[15] M. S. Skolnick and D. J. Mowbray, "Self-assembled semiconductor quantum dots: Fundamental physics and device applications," *Annu. Rev. Mater. Res.*, vol. 34, no. 1, pp. 181–218, 2004.

[16] F. Klopf, S. Deubert, J. P. Reithmaier, and A. Forchel, "Correlation between the gain profile and the temperature-induced shift in wavelength of quantum-dot lasers," *Appl. Phys. Lett.*, vol. 81, no. 2, pp. 217–219, 2002.

[17] T. D. Germann *et al.*, "Temperature-stable operation of a quantum dot semiconductor disk laser," *Appl. Phys. Lett.*, vol. 93, no. 5, p. 051104, 2008.

[18] O. Nasr *et al.*, "Carrier dynamics of strain-engineered InAs quantum dots with (In) GaAs surrounding material," *J. Opt.*, vol. 19, no. 2, p. 025401, 2017.

[19] M. Butkus *et al.*, "Quantum dot based semiconductor disk lasers for 1–1.3 μm," *IEEE J. Sel. Topics Quantum Electron.*, vol. 17, no. 6, pp. 1763–1771, Nov./Dec. 2011.

[20] D. A. Nakdali *et al.*, "High-power quantum-dot vertical-external-cavity surface-emitting laser exceeding 8 W," *IEEE Photon. Technol. Lett.*, vol. 26, no. 15, pp. 1561–1564, Aug. 5, 2014.

[21] M. Hoffmann *et al.*, "Femtosecond high-power quantum dot vertical external cavity surface emitting laser," *Opt. Exp.*, vol. 19, no. 9, pp. 8108–8116, 2011.

[22] A. Laurain *et al.*, "Influence of non-radiative carrier losses on pulsed and continuous VECSEL performance," *Proc. SPIE*, vol. 8242, p. 82420S, Feb. 2012.

[23] O. Sieber *et al.*, "Experimentally verified pulse formation model for high-power femtosecond VECSELs," (in English), *Appl. Phys. B, Lasers Opt.*, vol. 113, no. 1, pp. 133–145, 2013.

[24] M. Mangold *et al.*, "VECSEL gain characterization," *Opt. Exp.*, vol. 20, no. 4, pp. 4136–4148, 2012.

[25] G. J. Spühler *et al.*, "Semiconductor saturable absorber mirror structures with low saturation fluence," *Appl. Phys. B, Lasers Opt.*, vol. 81, no. 1, pp. 27–32, 2005.

[26] D. Waldburger, S. M. Link, C. G. Alfieri, M. Golling, and U. Keller, "High-power 100-fs SESAM-modelocked VECSEL," in *Proc. Lasers Congr. (ASSL, LSC, LAC)*, Boston, MA, USA, 2016, paper ATu1A.

[27] I. Kilen, S. W. Koch, J. Hader, and J. V. Moloney, "Non-equilibrium ultrashort pulse generation strategies in VECSELs," *Optica*, vol. 4, no. 4, pp. 412–417, Apr. 2017.

[28] I. J. Graumann *et al.*, "Peak-power scaling of femtosecond Yb:Lu_2O_3 thin-disk lasers," *Opt. Exp.*, vol. 25, no. 19, pp. 22519–22536, Sep. 2017.

[29] A. Laurain *et al.*, "Pulse interactions in a colliding pulse mode-locked vertical external cavity surface emitting laser," *J. Opt. Soc. Amer. B, Opt. Phys.*, vol. 34, no. 2, pp. 329–337, Feb. 2017.